Non Linear Parameter Varying Observer based on Descriptor Modeling for Damper Fault Estimation

Thanh-Phong Pham, Olivier Sename, Gia Quoc Bao Tran

Non Linear Parameter Varying Observer based on Descriptor Modeling for Damper Fault Estimation ⋆

Thanh-Phong Pham * **Olivier Sename** **
Gia Quoc Bao Tran **,***

* *Faculty of Electrical and Electronic Engineering, The University of Danang - University of Technology and Education, 550000 Danang, Vietnam (e-mail: ptphong@ute.udn.vn).*
** *Univ. Grenoble Alpes, CNRS, Grenoble INP⊤, GIPSA-Lab, 38000 Grenoble, France ⊤Institute of Engineering Univ. Grenoble Alpes (e-mail: olivier.sename@grenoble-inp.fr).*
*** *Centre Automatique et Systèmes (CAS), Mines Paris, Université PSL, 75006 Paris, France (e-mail: gia-quoc-bao.tran@minesparis.psl.eu).*

Abstract: This paper proposes an $\mathcal{H}_\infty$ Non Linear Parameter Varying (NLPV) observer for fault estimation in semi-active Electro-Rheological (ER) suspensions. The damper fault (a loss-of-efficiency factor) is modeled as a lost force of unknown/free dynamics to be estimated. Thanks to the parameter-dependent descriptor-form system modeling, there is no assumption made on the fault dynamics, thus making this method applicable to all considered types of damper faults. The nonlinearity in the damper model is bounded by its Lipschitz property, while the road disturbance and the measurement noise are handled using the $\mathcal{H}_\infty$ condition. The observer is parameterized and then designed by solving Linear Matrix Inequalities (LMIs) and is implemented in a polytopic gain scheduling approach. Synthesis results including Bode plots and simulations illustrate the method in both the frequency and the time domains.

Keywords: Descriptor form, NLPV observer, fault estimation, semi-active suspension, Lipchitz condition.

1. INTRODUCTION

In the automotive field, semi-active (SA) suspension systems are a potential candidate since they offer advantages in improving driving comfort with better performance than passive suspension and reduced energy consumption compared to active ones. There have been a lot of research, development, and implementation of such SA suspensions proposed in the literature (see (Savaresi et al., 2010) and references therein). Thorough reviews about these systems can be found in (Sename, 2021; Poussot-Vassal et al., 2012). It is worth noting that the loss of effectiveness of the SA suspension due to an electrical fault, physical deformation, or oil leakage may significantly reduce vehicle performances (Hernández-Alcántara et al., 2016; Morato et al., 2020). Therefore, fault detection of this system is of paramount importance for reliability.

For those purposes, a few studies have been concerned with the modeling of loss of effectiveness of the SA damper, as seen in (Hernández-Alcántara et al., 2016; Morato et al., 2020). Furthermore, some recent works have been dedicated to the study of damper fault estimation (Morato et al., 2019; Nguyen et al., 2016; Do et al., 2018; Tran et al., 2022). In these works, the loss of effectiveness of the damper is represented in the multiplicative or additive fault representations to develop a fault observer; however, the time derivative of the fault is assumed to be zero, which simplifies the theoretical problem but is not realistic for the considered system. Among fault estimation methods, the Proportional Integral (PI) observer (Do et al., 2018; Guzman et al., 2021) is interesting given that the fault varies very slowly and can then be modeled as a constant extra state. Besides, it is important to notice that the two main requirements concerning the development of the fault detection methods for the SA suspension are as follows: i) The schemes have to be able to deal with the bi-viscous nonlinearity in the SA suspension model; ii) The method must be able to handle the effect of unknown road profile disturbances and sensor noise on the estimation error.

To avoid making the slow-variation assumption of the fault dynamics and handle the requirements mentioned above, robust observers for descriptor Lipschitz systems are an interesting approach since the nonlinear function in the SA suspension model satisfies the global Lipschitz condition (see (6)). For the last two decades, many theoretical contributions to designing the observers for descriptor Lipschitz nonlinear systems have been proposed in the literature (Koenig, 2006; Darouach et al., 2011; Darouach and Boutat-Baddas, 2008; Darouach et al., 2017; Osorio-

⋆ This research is funded by Funds for Science and Technology Development of the University of Danang under project number B2020-DN06-21.

Gordillo et al., 2019; Ha and Trinh, 2004; Delshad et al., 2016). Those methods also account for disturbance minimization by mean of the $\mathcal{H}_\infty$, $\mathcal{H}_2$, or mixed $\mathcal{H}_\infty/\mathcal{H}_2$ criterion. Thus an $\mathcal{H}_\infty$ robust observer for singular nonlinear parameter-varying (NLPV) systems has been presented in (Do et al., 2020), but that method may be conservative due to assumptions such as bounded energy noise derivative.

In this paper, we consider the problem of estimating additive damper faults, represented by a loss of effectiveness, using accelerometers as inputs of the proposed observer only (to limit the cost over deflection sensors). To reduce the conservatism in (Do et al., 2020), an extension of (Delshad et al., 2016) is proposed using the $\mathcal{S}$-procedure to integrate the Lipschitz condition into the $\mathcal{H}_\infty$ condition. Our main contributions are summarized as follows:

- The semi-active suspension system is modeled as a descriptor NLPV formulation without any assumption on the fault dynamics;
- The results presented in (Delshad et al., 2016) to design a reduced-order observer are extended to a class of descriptor NLPV systems, for fault estimation;
- The proposed approach has been simulated on a quarter-car model built from our suspension testbed presented in (Pham et al., 2019). The observer performances are then assessed with simulation results in the time and frequency domain.

2. SEMI-ACTIVE SUSPENSION MODELING

An Electro-Rheological (ER) suspension system is illustrated in Fig. 1. More details about this system, as the model parameters given below and used for simulations are presented in (Pham et al., 2019).

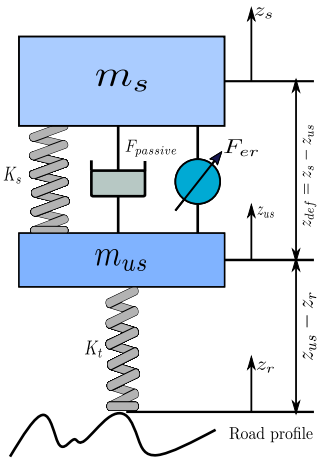

Fig. 1. Quarter-car model with semi-active suspension.

The well-known quarter-car model in Fig. 1 consists of the sprung mass m_s, the unsprung mass m_{us}, and the suspension components located between these masses and the tire which is modeled as a spring of stiffness k_t. From Newton's second law of motion, the system dynamics around the equilibrium are

$$\begin{cases} m_s \ddot{z}_s &= -F_s - F_d^f \\ m_{us}\ddot{z}_{us} &= F_s + F_d^f - F_t, \end{cases} \tag{1}$$

where $F_s = k_s z_{def}$ is the spring force ($z_{def} = z_s - z_{us}$ is the deflection); $F_t = k_t(z_{us} - z_r)$ is the tire force; the faulty damper force F_d^f is given in (3); z_s and z_{us} are the displacements of the sprung and unsprung masses, respectively; z_r is the road displacement input. The damper force F_d in the healthy case is as follows

$$\begin{cases} F_d &= \underbrace{k_0 z_{def} + c_0 \dot{z}_{def}}_{F_{passive}} + F_{er} \\ \dot{F}_{er} &= -\dfrac{1}{\tau}F_{er} + \dfrac{f_c}{\tau}\cdot u \cdot \tanh(k_1 z_{def} + c_1 \dot{z}_{def}), \end{cases} \tag{2}$$

where $u \in [0,1]$ is the control input signal representing the electric field supplied to the ER damper. Taking the loss of efficiency of the damper into account, the faulty damper force is

$$F_d^f = F_d - \alpha F_d = F_d - f, \tag{3}$$

where $\alpha \in [0,1]$ is the loss of effectiveness factor; f is the lost damper force to be estimated. It is remarkable that α is used to generate the lost damper force in the simulations. Substituting (3) into (1), we obtain the system dynamics considering the loss of effectiveness of the damper

$$\begin{cases} m_s \ddot{z}_s &= -F_s - F_d + f \\ m_{us}\ddot{z}_{us} &= F_s + F_d - f - F_t. \end{cases} \tag{4}$$

Choosing the state $x = (x_1, x_2, x_3, x_4, x_5, x_6)^\top = (z_s - z_{us}, \dot{z}_s, z_{us} - z_r, \dot{z}_{us}, F_{er}, f)^\top \in \mathbb{R}^6$, the measured output $y = (\ddot{z}_s, \ddot{z}_{us})^\top \in \mathbb{R}^2$, the scheduling variable $\rho = u \in [0,1]$, we rewrite the system dynamics in the descriptor NLPV form as

$$\begin{cases} E\dot{x} &= Ax + B(\rho)\Phi(Ex) + D_1\omega \\ y &= Cx + D_2\omega, \end{cases} \tag{5}$$

where $\omega = (\dot{z}_r \ \omega_n)^\top$, in which $\dot{z}_r$ is the road profile derivative and ω_n is the sensor noise.
The system nonlinearity $\Phi(Ex) = \tanh(k_1 x_1 + c_1(x_2 - x_4)) = \tanh(\Gamma_e x)$, with $\Gamma_e = (k_1 \ c_1 \ 0 \ -c_1 \ 0 \ 0)$, is globally Lipschitz, i.e., for all $(x, \hat{x}) \in \mathbb{R}^6 \times \mathbb{R}^6$,

$$\|\Phi(Ex) - \Phi(E\hat{x})\| \leq \|\Gamma_e(x - \hat{x})\|. \tag{6}$$

The matrices in (5) are (with $k = k_s + k_0$):

$$E = \begin{pmatrix} 1&0&0&0&0&0 \\ 0&1&0&0&0&0 \\ 0&0&1&0&0&0 \\ 0&0&0&1&0&0 \\ 0&0&0&0&1&0 \end{pmatrix}, B(\rho) = \begin{pmatrix} 0 \\ 0 \\ 0 \\ 0 \\ f_c\dfrac{\rho}{\tau} \end{pmatrix}, D_1 = \begin{pmatrix} 0&0 \\ 0&0 \\ -1&0 \\ 0&0 \\ 0&0 \end{pmatrix},$$

$$A = \begin{pmatrix} 0 & 1 & 0 & -1 & 0 & 0 \\ \dfrac{-k}{m_s} & \dfrac{-c_0}{m_s} & 0 & \dfrac{c_0}{m_s} & \dfrac{-1}{m_s} & \dfrac{1}{m_s} \\ 0 & 0 & 0 & 1 & 0 & 0 \\ \dfrac{k}{m_{us}} & \dfrac{c_0}{m_{us}} & \dfrac{-k_t}{m_{us}} & \dfrac{-c_0}{m_{us}} & \dfrac{1}{m_{us}} & \dfrac{-1}{m_{us}} \\ 0 & 0 & 0 & 0 & \dfrac{-1}{\tau} & 0 \end{pmatrix}, D_2 = \begin{pmatrix} 0 & 10^{-2} \\ 0 & 10^{-3} \end{pmatrix},$$

$$C = \begin{pmatrix} \dfrac{-k}{m_s} & \dfrac{-c_0}{m_s} & 0 & \dfrac{c_0}{m_s} & \dfrac{-1}{m_s} & \dfrac{1}{m_s} \\ \dfrac{k}{m_{us}} & \dfrac{c_0}{m_{us}} & \dfrac{-k_t}{m_{us}} & \dfrac{-c_0}{m_{us}} & \dfrac{1}{m_{us}} & \dfrac{-1}{m_{us}} \end{pmatrix}.$$

Note that here $\operatorname{rank}(E \ C)^\top = 6$.

Remark: Thanks to the descriptor system representation, the dynamics system taking the semi-active damper additive fault into account is presented without any assumption on the fault dynamics (unlike in Tran et al. (2022)).

3. NLPV OBSERVER DESIGN

In this Section, the reduced-order observer definition for descriptor systems (Delshad et al., 2016) is extended to a class of descriptor NLPV systems (5) as follows

$$\begin{cases} \dot{z} = N(\rho)z + J(\rho)y + H(\rho)\Phi(E\hat{x}) \\ \hat{x} = Rz + Sy, \end{cases} \tag{7}$$

where $z \in \mathbb{R}^{n_x - n_y}$ is the state variable of the reduced-order observer, $\hat{x}$ is the estimate of $x \in \mathbb{R}^{n_x}$, $y \in \mathbb{R}^{n_y}$ is the measurement, and $\rho \in \mathbb{R}^{n_\rho}$ is the scheduling parameter (here $n_x = 6$, $n_y = 2$, and $n_\rho = 1$). The observer matrices $N(\rho)$, $J(\rho)$, $H(\rho)$, R, and S of appropriate dimensions have to be designed. Let us introduce the dynamic error

$$\epsilon = z - TEx \in \mathbb{R}^{n_x - n_y}, \tag{8}$$

where the matrix T is an arbitrary matrix.

Differentiating (8) with respect to time and using (5) and (7), one obtains

$$\begin{cases} \dot{\epsilon} &= N(\rho)\epsilon + (N(\rho)T - TA + J(\rho)C)x \\ &\quad +(J(\rho)D_2 - TD_1)\omega + (H(\rho) - TB(\rho))\Phi(E\hat{x}) \\ &\quad -TB(\rho)(\Phi(Ex) - \Phi(\hat{E}x)) \\ \hat{x} &= R\epsilon + (RTE + SC)x + SD_2\omega. \end{cases} \tag{9}$$

It is obvious that if the decoupling conditions

$$N(\rho)TE - TA + J(\rho)C = 0, \tag{10}$$
$$H(\rho) - TB(\rho) = 0, \tag{11}$$
$$RTE + SC = I, \tag{12}$$

are satisfied, the system (9) becomes

$$\begin{cases} \dot{\epsilon} &= N(\rho)\epsilon - TB(\rho)\Delta\Phi + (J(\rho)D_2 - TD_1)\omega \\ e &= R\epsilon + SD_2\omega, \end{cases} \tag{13}$$

where $e = \hat{x} - x$ is the state estimation error and $\Delta\Phi = \Phi(Ex) - \Phi(E\hat{x})$.

The problem of the $\mathcal{H}_\infty$ observer design is thus reduced to determining the observer matrices $N(\rho)$, $J(\rho)$, $H(\rho)$, R, and S such that

- All the conditions (10)-(12) are satisfied;
- The effect of the combined disturbance-noise ω on the state estimation error e is minimized while $\Delta\Phi$ is bounded by the Lipschitz condition (6).

3.1 Parameterization of the Observer Matrices

First note that from (11), we get

$$H(\rho) = TB(\rho).$$

Therefore, $H(\rho)$ will be given when T is chosen. Now, in order to determine T and the observer matrices $N(\rho)$, $J(\rho)$, R, and S of the proposed observer satisfying all the conditions equalities (10)-(12), parameterization is made by using the general solution of (10) and (12).

First, from (10) and (12), one obtains

$$\begin{pmatrix} N(\rho) & J(\rho) \\ R & S \end{pmatrix} \begin{pmatrix} TE \\ C \end{pmatrix} = \begin{pmatrix} TA \\ I \end{pmatrix}. \tag{14}$$

The equation (14) is solvable if and only if

$$\operatorname{rank} \begin{pmatrix} TE \\ C \\ TA \\ I \end{pmatrix} = \operatorname{rank} \begin{pmatrix} TE \\ C \end{pmatrix} = n_x. \tag{15}$$

Next, let $M \in \mathbb{R}^{n_x \times n_x}$ be an arbitrary matrix of full row rank such that

$$\operatorname{rank} \begin{pmatrix} M \\ C \end{pmatrix} = \operatorname{rank} \begin{pmatrix} TE \\ C \end{pmatrix} = n_x. \tag{16}$$

Then there always exists a parameter matrix K such that

$$\begin{pmatrix} TE \\ C \end{pmatrix} = \begin{pmatrix} I & -K \\ 0 & I \end{pmatrix} \begin{pmatrix} M \\ C \end{pmatrix} \iff TE = M - KC$$
$$\iff (T \ K) \begin{pmatrix} E \\ C \end{pmatrix} = M. \tag{17}$$

A solution for (16) is given by

$$(T \ K) = M\Sigma^+, \tag{18}$$

where $\Sigma = (E \ C)$ where Σ^+ is any general inverse of matrix Σ satisfying $\Sigma\Sigma^+\Sigma = \Sigma$. This is equivalent to

$$T = M\Sigma^+ \begin{pmatrix} I \\ 0 \end{pmatrix}, \quad K = M\Sigma^+ \begin{pmatrix} 0 \\ I \end{pmatrix}. \tag{19}$$

Besides, the solution set of (14) is given by

$$\begin{pmatrix} N(\rho) & J(\rho) \\ R & S \end{pmatrix} = \begin{pmatrix} TA \\ I \end{pmatrix} \begin{pmatrix} TE \\ C \end{pmatrix}^+ + \begin{pmatrix} Z_1(\rho) \\ Z_2 \end{pmatrix} \left(I - \begin{pmatrix} TE \\ C \end{pmatrix} \begin{pmatrix} TE \\ C \end{pmatrix}^+ \right), \tag{20}$$

where $\begin{pmatrix} Z_1(\rho) \\ Z_2 \end{pmatrix}$ is a free matrix of appropriate dimension. This is equivalent to

$$N(\rho) = TA\alpha_1 + Z_1(\rho)\beta_1, \tag{21}$$
$$J(\rho) = TA\alpha_2 + Z_1(\rho)\beta_2, \tag{22}$$
$$R = \alpha_1 + Z_2\beta_1, \tag{23}$$
$$S = \alpha_2 + Z_2\beta_2, \tag{24}$$

where $\alpha_1 = \begin{pmatrix} TE \\ C \end{pmatrix}^+ \begin{pmatrix} I \\ 0 \end{pmatrix}$, $\alpha_2 = \begin{pmatrix} TE \\ C \end{pmatrix}^+ \begin{pmatrix} 0 \\ I \end{pmatrix}$,

$\beta_1 = \left(I - \begin{pmatrix} TE \\ C \end{pmatrix} \begin{pmatrix} TE \\ C \end{pmatrix}^+ \right) \begin{pmatrix} I \\ 0 \end{pmatrix}$, and

$\beta_2 = \left(I - \begin{pmatrix} TE \\ C \end{pmatrix} \begin{pmatrix} TE \\ C \end{pmatrix}^+ \right) \begin{pmatrix} 0 \\ I \end{pmatrix}$.

Remark: If the matrices $N(\rho)$, $J(\rho)$, $H(\rho)$, R, and S can be chosen according to (21), (22), (11), (23), and (24), respectively, then all conditions (10)-(12) are fulfilled.

From the results of the parameterization above, for brevity, the matrices of the system (13) can be rewritten as

$$\mathbb{A}(\rho) = N(\rho) = A_{11} + Z_1(\rho)A_{12}, \tag{25}$$
$$\mathbb{B}(\rho) = J(\rho)D_2 - TD_1 = B_{11} + Z_1(\rho)B_{12}, \tag{26}$$
$$\mathbb{W}(\rho) = -TB(\rho), \tag{27}$$
$$\mathbb{C} = R = C_{11} + Z_2C_{12}, \tag{28}$$
$$\mathbb{D} = SD_2 = D_{11} + Z_2D_{12}, \tag{29}$$

where $A_{11} = TA\alpha_1$, $A_{12} = \beta_1$, $B_{11} = TA\alpha_2D_2 - TD_1$, $B_{12} = \beta_2D_2$, $C_{11} = \alpha_1$, $C_{12} = \beta_1$, $D_{11} = \alpha_2D_2$, and $D_{12} = \beta_2D_2$. Notice that all the matrices A_{11}, A_{12}, B_{11}, B_{12}, C_{11}, C_{12}, D_{11}, and D_{12} are known and the matrix $\mathbb{W}(\rho)$ is known at each vertex of ρ. Therefore, the observer design problem is reduced to determining $Z_1(\rho)$ and Z_2, which is discussed in the following part.

3.2 Polytopic $\mathcal{H}_\infty$ Observer Design

Using (25)-(29), we rewrite the estimation error dynamics (13) as

$$\begin{cases} \dot{\epsilon} &= \mathbb{A}(\rho)\epsilon + \mathbb{W}(\rho)\Delta\Phi + \mathbb{B}(\rho)\omega \\ e &= \mathbb{C}\epsilon + \mathbb{D}\omega. \end{cases} \tag{30}$$

After the parameterization step, while $\Delta\Phi$ is bounded by the Lipschitz condition (6), the observer design problem is now to determine the matrices $Z_1(\rho)$ and Z_2 such that

- The system (30) is asymptotically stable for $\omega(t) = 0$;
- $\|e(t)\|_{\mathcal{L}_2} < \gamma\|\omega(t)\|_{\mathcal{L}_2}$ for $\omega(t) \neq 0$; γ is minimized.

In this paper, the design of the observer will be carried out using the polytopic method. It means that we assume that $Z_1(\rho)$ depends in an affine way on the parameter ρ. In such a case, the design method is restricted to solving the given problem only to get the vertices $Z_{1,i}$ of $Z_1(\rho)$ formed when ρ varies within its bounds (Apkarian et al., 1995). Theorem 1 then solves the observer design problem in an LMI framework.

Theorem 1. Consider the system model (5) and the observer (7). The observer design problem is solved if there exist matrices $X = X^\top > 0$, Y_i, Z_2, and a scalar $\kappa > 0$ minimizing γ such that

$$\begin{pmatrix} \Omega_{11,i} & X\mathbb{W}(\rho_i) & \Omega_{13,i} & \Omega_{14} & \Omega_{15} \\ \mathbb{W}^\top(\rho_i)X & -\kappa I & 0 & 0 & 0 \\ \Omega_{13,i}^\top & 0 & -\gamma^2 I & \Omega_{34} & \Omega_{35} \\ \Omega_{14}^\top & 0 & \Omega_{34}^\top & -I & 0 \\ \Omega_{15}^\top & 0 & \Omega_{35}^\top & 0 & -\kappa I \end{pmatrix} < 0, \tag{31}$$

for $\rho_i, i = 1, 2, \ldots, 2^{n_\rho}$ at the 2^{n_ρ} vertices of ρ, where $\Omega_{11,i} = A_{11}^\top X + XA_{11} + A_{12}^\top Y_i^\top + Y_i A_{12}$; $\Omega_{13,i} = XB_{11} + Y_i B_{12}$; $\Omega_{14} = C_{11}^\top + C_{12}^\top Z_2^\top$; $\Omega_{15} = C_{11}^\top \Gamma_e^\top + C_{12}^\top Z_2^\top \Gamma_e$; $\Omega_{34} = D_{11}^\top + D_{12}^\top Z_2^\top$; $\Omega_{35} = D_{11}^\top \Gamma_e^\top + D_{12}^\top Z_2^\top \Gamma_e^\top$. Then, $Z_{1,i}$ for each vertex of ρ is found as $Z_{1,i} = -X^{-1}Y_i$.

Proof. Consider the Lyapunov function candidate

$$V = \epsilon^\top X \epsilon. \tag{32}$$

Differentiating V along the solution of (30) yields

$$\begin{aligned} \dot{V} &= \dot{\epsilon}^\top X\epsilon + \epsilon^\top X\dot{\epsilon} \\ &= (\mathbb{A}(\rho)\epsilon + \mathbb{W}(\rho)\Delta\Phi + \mathbb{B}(\rho)\omega)^\top X\epsilon \\ &\quad + \epsilon^\top X(\mathbb{A}(\rho)\epsilon + \mathbb{W}(\rho)\Delta\Phi + \mathbb{B}(\rho)\omega). \end{aligned} \tag{33}$$

To satisfy the performance objective with respect to the $\mathcal{L}_2$ gain disturbance attenuation, we must satisfy the inequality

$$\begin{aligned} &\dot{V} + e^\top e - \gamma^2\omega^\top\omega < 0 \iff \\ &\epsilon^\top(\mathbb{A}(\rho)^\top X + X\mathbb{A}(\rho) + \mathbb{C}^\top\mathbb{C})\epsilon + \Delta\Phi^\top\mathbb{W}^\top(\rho)X\epsilon \\ &+ \epsilon^\top X\mathbb{W}(\rho)\Delta\Phi + \omega^\top(\mathbb{B}(\rho)^\top X + \mathbb{D}^\top\mathbb{C})\epsilon \\ &+ \epsilon^\top(X\mathbb{B}(\rho) + \mathbb{C}^\top\mathbb{D})\omega + \omega^\top(\mathbb{D}^\top\mathbb{D} - \gamma^2 I)\omega < 0. \end{aligned} \tag{34}$$

Defining $\eta = \begin{pmatrix} \epsilon \\ \Delta\Phi \\ \omega \end{pmatrix}$, one obtains

$$\dot{V} = \eta^\top Q_1(\rho)\eta < 0, \tag{35}$$

where $Q_1(\rho) = \begin{pmatrix} \Omega(\rho) & X\mathbb{W}(\rho) & X\mathbb{B}(\rho) + \mathbb{C}^\top\mathbb{D} \\ \mathbb{W}^\top(\rho)X & 0 & 0 \\ \mathbb{B}(\rho)^\top X + \mathbb{D}^\top\mathbb{C} & 0 & \mathbb{D}^\top\mathbb{D} - \gamma^2 I \end{pmatrix}$,

where $\Omega(\rho) = \mathbb{A}(\rho)^\top X + X\mathbb{A}(\rho) + \mathbb{C}^\top\mathbb{C}$.

From (6), the following condition is obtained

$$\begin{aligned} &(\Phi(Ex) - \Phi(E\hat{x}))^\top(\Phi(Ex) - \Phi(E\hat{x})) \leqslant e^\top\Gamma_e^\top\Gamma_e e \\ \iff &(\Delta\Phi)^\top\Delta\Phi \leqslant (\mathbb{C}\epsilon + \mathbb{D}\omega)^\top\Gamma_e^\top\Gamma_e(\mathbb{C}\epsilon + \mathbb{D}\omega) \\ \iff &\eta^\top Q_2\eta \leqslant 0, \end{aligned} \tag{36}$$

where $Q_2 = \begin{pmatrix} -\mathbb{C}^\top\Gamma_e^\top\Gamma_e\mathbb{C} & 0 & -\mathbb{C}^\top\Gamma_e^\top\Gamma_e\mathbb{D} \\ 0 & I & 0 \\ -\mathbb{D}^\top\Gamma_e^\top\Gamma_e\mathbb{C} & 0 & -\mathbb{D}^\top\Gamma_e^\top\Gamma_e\mathbb{D} \end{pmatrix}$.

By applying the $\mathcal{S}$-procedure (Boyd et al., 1994) to the inequalities (35) and (36), we have that $\dot{V} + e^\top e - \gamma^2\omega^\top\omega < 0$ if there exists a scalar $\kappa > 0$ such that

$$\begin{aligned} &\dot{V} + e^\top e - \gamma^2\omega^\top\omega - \kappa(\eta^\top Q\eta) < 0 \\ \iff &\eta^\top(Q_1(\rho) - \kappa Q_2)\eta < 0. \end{aligned} \tag{37}$$

The condition (37) is equivalent to

$$\begin{aligned} &Q_1(\rho) - \kappa Q_2 < 0 \\ \iff &\begin{pmatrix} \Omega_a(\rho) & X\mathbb{W}(\rho) & \Omega_b(\rho) \\ \mathbb{W}^\top(\rho)X & -\kappa I & 0 \\ \Omega_b(\rho)^\top & 0 & \Omega_c \end{pmatrix} < 0, \end{aligned} \tag{38}$$

where $\Omega_a(\rho) = \mathbb{A}(\rho)^\top X + X\mathbb{A}(\rho) + \mathbb{C}^\top\mathbb{C} + \kappa\mathbb{C}^\top\Gamma_e^\top\Gamma_e\mathbb{C}$, $\Omega_b = X\mathbb{B}(\rho) + \mathbb{C}^\top\mathbb{D} + \kappa\mathbb{C}^\top\Gamma_e^\top\Gamma_e\mathbb{D}$, and $\Omega_c = \mathbb{D}^\top\mathbb{D} + \kappa\mathbb{D}^\top\Gamma_e^\top\Gamma_e\mathbb{D} - \gamma^2 I$.

Applying Schur's complement to (38), one obtains

$$\begin{pmatrix} \Omega_1(\rho) & X\mathbb{W}(\rho) & X\mathbb{B}(\rho) & \mathbb{C}^\top & \mathbb{C}^\top\Gamma_e^\top \\ \mathbb{W}^\top(\rho)X & -\kappa I & 0 & 0 & 0 \\ \mathbb{B}^\top X & 0 & -\gamma^2 I & \mathbb{D}^\top & \mathbb{D}^\top\Gamma_e^\top \\ \mathbb{C} & 0 & \mathbb{D} & -I & 0 \\ \Gamma_e\mathbb{C} & 0 & \Gamma_e\mathbb{D} & 0 & -\kappa I \end{pmatrix} < 0, \tag{39}$$

where $\Omega_1(\rho) = \mathbb{A}(\rho)^\top X + X\mathbb{A}(\rho)$.

Substituting (25)-(29) into (39) and letting $Y_i = -XZ_{1,i}$ with $Z_{1,i} = Z_1(\rho_i)$ at each vertex ρ_i of ρ, we obtain the LMI (31) at the vertex ρ_i.

If (31) is satisfied, from (36), (37) implies that

$$\dot{V} + e^\top e - \gamma^2\omega^\top\omega < 0. \tag{40}$$

Following the steps in (Darouach et al., 2011), we get

$$\|e(t)\|_{\mathcal{L}_2}^2 < \gamma^2\|\omega(t)\|_{\mathcal{L}_2}^2. \tag{41}$$

The proof is completed. □

After solving Theorem 1 for the 2 vertices of $Z_1(\rho)$ and for Z_2, we solve (21), (22), (11), (23), and (24) for the observer matrices (at the vertices), then the polytopic convex computation of the matrix gain is used in implementation (Apkarian et al., 1995).

4. OBSERVER SYNTHESIS RESULTS

In this Section, the synthesis results of the NLPV observer are shown. First, the observer proposed in Section 3 is designed for the system presented in Section 2. Solving Theorem 1, so the LMIs (31) with vertices $\rho_1 = 0$ and $\rho_2 = 1$, we obtain the minimum $\mathcal{L}_2$-induced gain $\gamma = 2.0078$, $\kappa = 160$, and the matrices $Z_{1,i}, i = 1, 2$ and Z_2. According to (21)-(24) the observer matrices at each vertex are obtained as follows: $N_i = TA\alpha_1 + Z_{1,i}\beta_1$, $J_i = TA\alpha_2 + Z_{1,i}\beta_2$, for $i = 1, 2$, $R = \alpha_1 + Z_2\beta_1$, and $S = \alpha_2 + Z_2\beta_2$. Then the observer matrices $N(\rho)$ and $J(\rho)$ are deduced by using convex interpolation.

In Fig. 2 and Fig. 3, the Bode diagrams of the estimation error systems with respect to the road profile derivative and sensor noise are shown for the two vertex observers for parameter values $\rho = \{0, 1\}$. These results emphasize the satisfactory attenuation level (typically of the range -50 to -100 dB) of the unknown road profile derivative, and of measurement noise appearing at high frequencies, on the six estimation errors e with scheduling parameter $\rho_1 = 0$ (red dashed line) and $\rho_2 = 1$ (blue line).

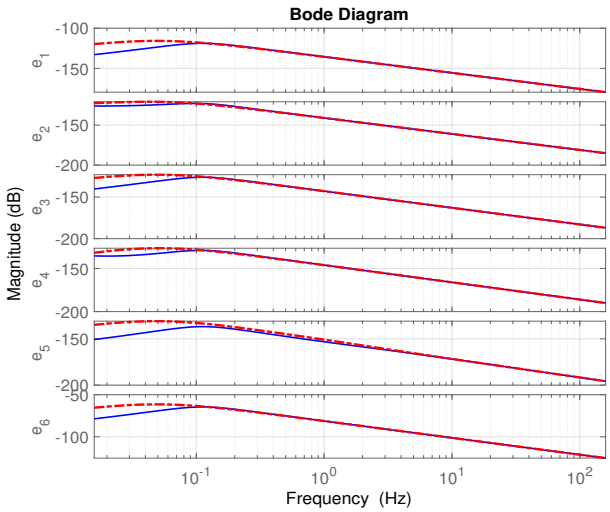

Fig. 2. Transfer $\|e/\dot{z}_r\|$—Bode diagrams of NLPV observer with respect to the road profile derivative with $\rho_1 = 0$ (red dashed line) and $\rho_2 = 1$ (blue line).

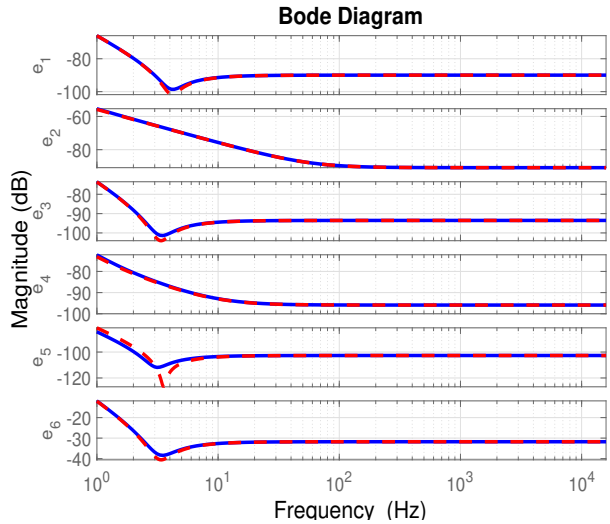

Fig. 3. Transfer $\|e/\omega_n\|$—Bode diagrams of NLPV observer with respect to the measurement noise with $\rho_1 = 0$ (red dashed line) and $\rho_2 = 1$ (blue line).

5. SIMULATION RESULTS

To emphasize the effectiveness of the proposed approach, simulations are now performed considering the nonlinear quarter-car model (5). The initial conditions are $x(0) = (0\ 0\ 0\ 0\ 0\ 0)^\top$ for the system and $z(0) = (0\ 0.01\ 0.2\ 1)^\top$ for the reduced-order observer.

Two simulation scenarios are used to evaluate the performance of the observer as follows.

Simulation 1:

- The road profile is sinusoidal;
- The control u (recall $\rho = u$) is constant at $u = 0.3$;
- α (as in (3)) increases from 0 to 0.2 at 7s.

Simulation 2:

- An ISO 8608 road profile of Type C is used;
- The control u is obtained from a Skyhook controller. It is important to note that in such a case, u varies infinitely fast, which means that the use of the polytopic approach is justified;
- α increases from 0 to 0.2 at 5s and then to 0.4 at 10s.

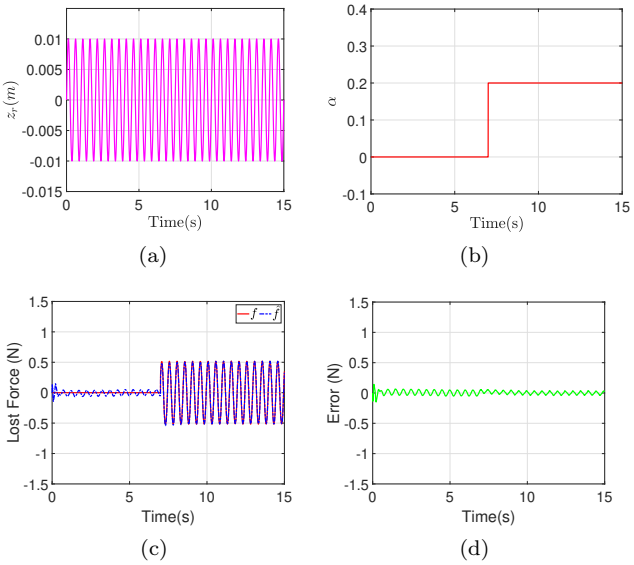

Fig. 4. Simulation 1: (a) Road profile, (b) Loss-of-efficiency factor, (c) Fault estimation, and (d) Estimation error.

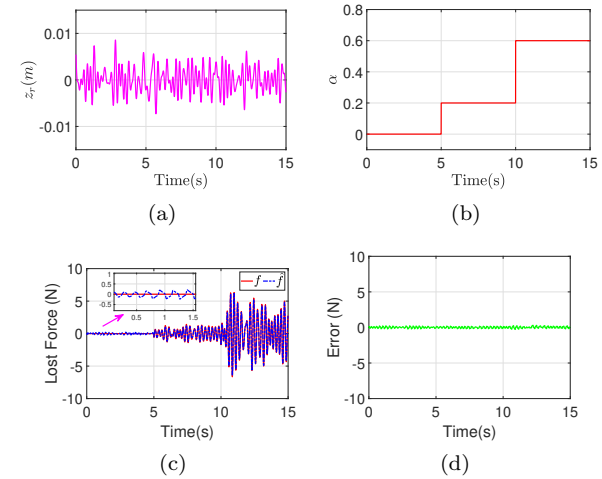

Fig. 5. Simulation 2: (a) Road profile, (b) Loss-of-efficiency factor, (c) Fault estimation, and (d) Estimation error.

The simulation results are shown in Fig. 4 and Fig. 5. It can be seen that the asymptotic estimation is achieved with small errors (see Table 1) and for various kinds of variations in the fault, which highlights the advantage that our method is appropriate for all fault dynamics.

Table 1. Normalized Root-Mean-Square Errors (NRMSE).

Simulation	NRMSE (-)
Scenario 1	0.0315
Scenario 2	0.0091

6. CONCLUSION

This paper presents an NLPV observer to estimate the damper fault (modeled as the lost damper force) in SA ER automotive suspensions. The descriptor NLPV modeling avoids any assumption made on the fault dynamics, making the approach suitable for any faults. While the Lipschitz condition is used to bound the system nonlinearity, the combined effects of unknown inputs (road profile derivative and measurement noise) on the estimation error are minimized using the $\mathcal{H}_\infty$ condition. Both frequency-domain analysis and time-domain simulations assess the performance of the method.

REFERENCES

Apkarian, P., Gahinet, P., and Becker, G. (1995). Self-scheduled H_∞ Control of Linear Parameter-varying Systems: A Design Example. *Automatica*, 31(9), 1251–1261.

Boyd, S., El Ghaoui, L., Feron, E., and Balakrishnan, V. (1994). *Linear Matrix Inequalities in System and Control Theory*, volume 15. Siam.

Darouach, M. and Boutat-Baddas, L. (2008). Observers for a Class of Nonlinear Singular Systems. *IEEE Transactions on Automatic Control*, 53(11), 2627–2633. doi:10.1109/TAC.2008.2007868.

Darouach, M., Amato, F., and Alma, M. (2017). Functional Observers Design for Descriptor Systems via LMI: Continuous and Discrete-time Cases. *Automatica*, 86, 216–219. doi: https://doi.org/10.1016/j.automatica.2017.08.016.

Darouach, M., Boutat-Baddas, L., and Zerrougui, M. (2011). H_∞ Observers Design for a Class of Nonlinear Singular Systems. *Automatica*, 47(11), 2517–2525.

Delshad, S.S., Johansson, A., Darouach, M., and Gustafsson, T. (2016). Robust State Estimation and Unknown Inputs Reconstruction for a Class of Nonlinear Systems: Multiobjective Approach. *Automatica*, 64, 1–7.

Do, M.H., Koenig, D., and Theilliol, D. (2018). Robust H∞ Proportional-Integral Observer for Fault Diagnosis: Application to Vehicle Suspension. *IFAC-PapersOnLine*, 51(24), 536–543. doi: https://doi.org/10.1016/j.ifacol.2018.09.628. 10th IFAC Symposium on Fault Detection, Supervision and Safety for Technical Processes SAFEPROCESS 2018.

Do, M.H., Koenig, D., and Theilliol, D. (2020). H∞ Observer Design for Singular Nonlinear Parameter-varying System. In *2020 59th IEEE Conference on Decision and Control (CDC)*, 3927–3932. doi: 10.1109/CDC42340.2020.9303844.

Guzman, J., López-Estrada, F.R., Estrada-Manzo, V., and Valencia-Palomo, G. (2021). Actuator Fault Estimation based on a Proportional-integral Observer with Non-quadratic Lyapunov Functions. *International Journal of Systems Science*, 1–14.

Ha, Q.P. and Trinh, H. (2004). State and Input Simultaneous Estimation for a Class of Nonlinear Systems. *Automatica*, 40(10), 1779–1785.

Hernández-Alcántara, D., Tudón-Martínez, J.C., Amézquita-Brooks, L., Vivas-López, C.A., and Morales-Menéndez, R. (2016). Modeling, Diagnosis and Estimation of Actuator Faults in Vehicle Suspensions. *Control Engineering Practice*, 49, 173–186. doi: https://doi.org/10.1016/j.conengprac.2015.12.002.

Koenig, D. (2006). Observers Design for Unknown Input Nonlinear Descriptor Systems via Convex Optimization. *IEEE Transactions on Automatic control*, (06), 1047–1052.

Morato, M.M., Sename, O., Dugard, L., and Nguyen, M.Q. (2019). Fault Estimation for Automotive Electro-Rheological Dampers: LPV-based Observer Approach. *Control Engineering Practice*, 85, 11–22. doi: https://doi.org/10.1016/j.conengprac.2019.01.005.

Morato, M., Pham, T.P., Sename, O., and Dugard, L. (2020). Development of a Simple ER Damper Model for Fault-tolerant Control Design. *Journal of the Brazilian Society of Mechanical Sciences and Engineering*, 42(10), 502 (2020). doi:10.1007/s40430-020-02585-y.

Nguyen, M.Q., Sename, O., and Dugard, L. (2016). Comparison of Observer Approaches for Actuator Fault Estimation in Semi-active Suspension Systems. In *2016 3rd Conference on Control and Fault-Tolerant Systems (SysTol)*, 227–232. IEEE.

Osorio-Gordillo, G.L., Darouach, M., Astorga-Zaragoza, C.M., and Boutat-Baddas, L. (2019). Generalised Dynamic Observer Design for Lipschitz Non-linear Descriptor Systems. *IET Control Theory & Applications*, 13(14), 2270–2280.

Pham, T.P., Sename, O., and Dugard, L. (2019). Unified $\mathcal{H}_\infty$ Observer for a Class of Nonlinear Lipschitz Systems: Application to a Real ER Automotive Suspension. *IEEE Control Systems Letters*, 3(4), 817–822. doi: 10.1109/LCSYS.2019.2919813.

Poussot-Vassal, C., Spelta, C., Sename, O., Savaresi, S.M., and Dugard, L. (2012). Survey and Performance Evaluation on some Automotive Semi-active Suspension Control Methods: A Comparative Study on a Single-corner Model. *Annual Reviews in Control*, 36(1), 148–160.

Savaresi, S.M., Poussot-Vassal, C., Spelta, C., Sename, O., and Dugard, L. (2010). *Semi-active Suspension Control Design for Vehicles*. Elsevier.

Sename, O. (2021). Review on LPV Approaches for Suspension Systems. *Electronics*, 10(17), 2120.

Tran, G.Q.B., Pham, T.P., and Sename, O. (2022). Multi-objective Grid-based Lipschitz NLPV PI Observer for Damper Fault Estimation. In *11th IFAC Symposium on Fault Detection, Supervision and Safety for Technical Processes - SAFEPROCESS 2022*. Paphos, Cyprus. URL `https://hal.archives-ouvertes.fr/hal-03611561`.